Cancer Nano (2011) 2:67–79
DOI 10.1007/s12645-011-0017-5

ORIGINAL PAPER

Effect of liposomal celecoxib on proliferation of colon cancer cell and inhibition of DMBA-induced tumor in rat model

Venkatesan Perumal · Shubhadeep Banerjee · Shubasis Das · R. K. Sen · Mahitosh Mandal

Received: 22 April 2011 / Accepted: 29 June 2011 / Published online: 13 July 2011

Abstract Celecoxib, a selective cyclooxygenase-2 inhibitor, has shown potential anticancerous activity against majority of solid tumors especially on patients with colon cancer. However, associations of serious side effects limit the usage of celecoxib in colon cancer treatment. To address this issue and provide an alternative strategy to increase the efficacy of celecoxib, liposomal formulation of celecoxib was prepared and characterized. Anticancer activity of liposomal celecoxib on colon cancer cell HCT 15 was evaluated in vitro. Furthermore, tumor inhibition efficiency by liposomal celecoxib was studied on 7,12-dimethyl benz (a)anthracene (DMBA)-induced tumor in rat model. In order to elucidate the antioxidant activity of celecoxib-loaded liposomes, antioxidant superoxide dismutase (SOD) generation and lipid peroxide (LPx) formation in both liver and kidney tissues were examined. Characterization of the formed unilamellar liposomes revealed the formation of homogeneous suspension of neutral (empty) or anionic (celecoxib-loaded) liposomes with a well-defined spherical shape which have a mean size of 103.5 nm (empty liposome) and 169 nm (liposomal celecoxib). High-performance liquid chromatography (HPLC) analysis and hemolytic assay demonstrated 46% of celecoxib entrapment efficiency and significantly low hemolysis, respectively. Liposomal celecoxib exhibited dose-dependent cytotoxicity and apoptotic activity against HCT 15 cells which are comparable to free celecoxib. In vivo study demonstrated inhibition of tumor growth. Biochemical analysis of the liposomal celecoxib-treated group significantly inhibited the LPx formation (oxygen-free radicals) and increased the activity of SOD. Our results present the potential of inhibiting colon cancer in vitro and DMBA-induced tumor in rat model in vivo by liposomal celecoxib.

Keywords Liposomes · Celecoxib · Colon cancer · Hemocompatibilty · Cytotoxicity

V. Perumal · S. Banerjee · M. Mandal (✉)
School of Medical Science and Technology,
Indian Institute of Technology,
Kharagpur, India 721302
e-mail: mahitosh@smst.iitkgp.ernet.in

S. Das · R. K. Sen
Department of Biotechnology, Indian Institute of Technology,
Kharagpur, India 721302

V. Perumal
Nanotech Research Facility,
PSG Institute of Advanced Studies (PSGIAS),
Coimbatore, India 641 004

1 Introduction

Chemotherapeutic agents used for cancer treatment have large volume of distribution upon intravenous administrations which result in narrow therapeutic index, unsolicited drug distribution, and high level of toxicity in healthy tissues (Turanek et al. 2009). In the recent years, several research works have manipulated pharmacokinetic and biodistribution properties of drug-loaded lipid/polymer nanocarriers to improve the anticancer activity (Yang et al. 2007; Lu et al. 2008; Nakano et al. 2008; Hiremath et al. 2009). The nanocarriers should be long circulating in blood in order to passively target tumor tissue through enhanced permeability and retention effect (EPR) (Katanasaka et al. 2008). Among the several nanocarriers, liposomes are extensively used for drug delivery and modeling of cell membrane to elucidate their endocytosis mechanisms (Nakano et al. 2008; Hiremath et al. 2009). Liposomes are sophisticated and handy nanodelivery systems which

facilitate targeted drug delivery, thereby reducing organ-specific side effects of several anticancer agents (Abu Lila et al. 2009). Liposomal formulation of hydrophobic drugs has been reported to overcome the solubility and the solvent-induced side effects (Katanasaka et al. 2008). In vivo studies using liposomal formulations have also been reported to reduce anticancer agent-mediated toxicities (Storm et al. 1987; Turanek et al. 2009). Indeed, the liposomal formulation of anticancer agents approved for medical applications are daunorubicin (DaunoXome) and DOX (Doxil; Drummond et al. 1999). Liposomal formulation of paclitaxel and doxorubicin are the prime examples for enhanced solubility and reduced cardiotoxicity profile, respectively (Yang et al. 2007; Tan et al. 2010).

Among the different types of cancer, colon cancer is the second leading cause of cancer-related deaths worldwide. According to the World Health Organization (WHO) report, colon cancer accounts for 677,000 deaths per year (Auman et al. 2008). Commonly used first-line chemotherapeutic regimens for colon cancer involve combination of infusional 5-fluorouracil, leucovorin, and oxaliplatin with bevacizumab or infusional 5-fluorouracil, leucovorin, and irinotecan with bevacizumab (Gaiser et al. 2008). Despite the chemotherapy, solubility and organ-specific toxicity associated with several anticancer agents necessitate designing effective formulation to treat colon cancer.

Within the family of non-steroidal anti-inflammatory drugs, celecoxib has been most frequently investigated for its anticancer activity against various in vitro and in vivo models (Hsiao et al. 2007; Bijman et al. 2008; Dhawan et al. 2008; Fig. 1a). Preclinical studies using celecoxib have reported prominent anticancer activity against head and neck squamous cell carcinoma, colon cancer, breast cancer, and lung cancer (Hsiao et al. 2007; Bijman et al. 2008). Despite the approval of celecoxib (oral administration) by FDA (Food and Drug Adminstration) of USA for adjuvant therapy in patients with familial adenomatous polyposis and precancerous disease of colon, association of greater intensity of side effects (thromboembolism and cardiovascular risk) and poor water solubility limit its usage in cancer therapy (Mazhar et al. 2006; Mohammed et al. 2006; Auman et al. 2008). It has also been reported that celecoxib is rapidly eliminated from plasma which limits therapeutic concentration of celecoxib at tumor sites (Paulson et al. 2000, 2001). Therefore, it is more essential to find alternative method

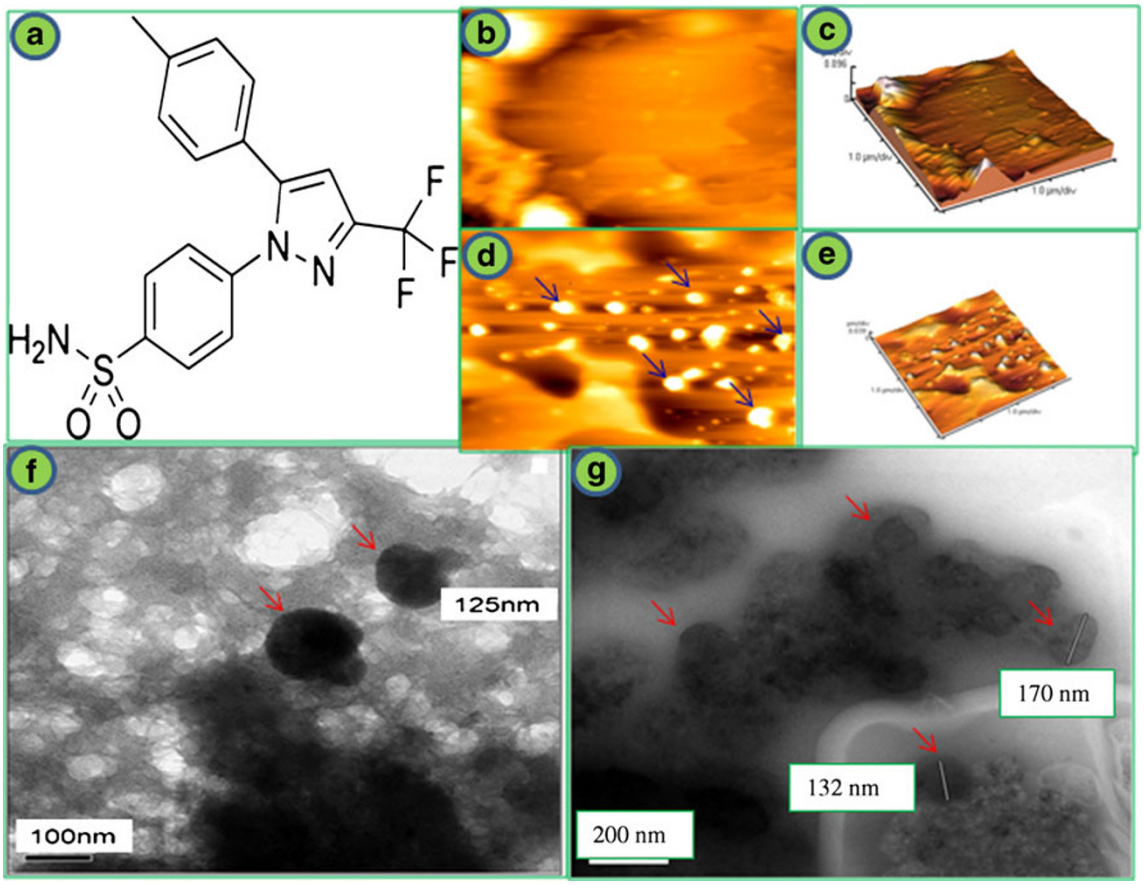

Fig. 1 **a** Structure of celecoxib; AFM images of **b** and **c** empty liposomes and **d** and **e** celecoxib-loaded liposomes; TEM images of **f** empty liposomes and **g** celecoxib-loaded liposomes

for celecoxib administration, i.e., specific drug delivery systems to reduce the side effects and to increase anticancer activity. So, it is hypothesized that liposomal formulation of celecoxib might provide a novel approach to circumvent the poor solubility, to improve the therapeutic index, and to diminish cardiotoxicity induced by celecoxib (Maier et al. 2004; Hsiao et al. 2007; Sakoguchi-Okada et al. 2007; Bijman et al. 2008; Gaiser et al. 2008). To the best of our knowledge, no studies have been reported using effect of liposomal celecoxib on colon cancer. In view of the above, liposomal celecoxib was prepared and characterized for morphology, size, zeta potential, entrapment efficiency, and hemocompatibility. Anticancer activity of liposomal celecoxib was analyzed by cell proliferation assay, morphological, cell cycle, and apoptosis analysis. Furthermore, tumor inhibitory effect of liposomal celecoxib was evaluated on DMBA-induced rat tumor model.

2 Materials and methods

DSPC (1,2-distearoyl-*sn*-glycero-phosphatidylcholine), MTT (3-(4,5-dimethyltiazol-2-yl)-2,5-diphenyltetrazolium bromide), PI (propidium iodide), DAPI (4′,6-diamidino-2-phenylindole), reduced glutathione, DTNB (5,5-dithiobis (2-nitrobenzoic acid)), RNase (ribonuclease), and DMBA were obtained from Sigma Aldrich, USA. Synthetic grade of methanol and chloroform was obtained from Merck, India. Celecoxib was generously provided by Aarthi Drug Ltd, Mumbai, India. HEPES was obtained from Sisco Research Labs. Animal food pellet was supplied by Hindustan Lever Ltd, Mumbai, India. Phosphotungstic acid, thiobarbituric acid, trichloroacetic acid, acetic acid, sodium salicylate, and EDTA were purchased from the Himedia Chemicals (Pvt) Ltd, Mumbai, India. Ascorbate, $FeCl_3$, sodium tungstate, sodium nitrate, methanol, and other reagents were of analytical grade. All other chemicals were of highest possible grade and obtained from commercial sources. The chemicals were used as supplied.

2.1 Cell culture and conditions

Human colon cancer cell line HCT 15 (National Centre for Cell Science (NCCS), Pune, India) was grown as adherent culture in RPMI 1640 medium (Himedia, India) supplemented with 10% FBS (Gibco®, Invitrogen, India), 2 mM L-glutamine, 100 units/ml penicillin, and 0.1 mg/ml streptomycin (Himedia, India) at 37°C and 5% CO_2 in air. After the cells became 80% confluent (usually after 3 days), they were trypsinized (0.25% trypsin+0.1% EDTA), centrifuged (Heraeus table top centrifuge E003) and suspended in medium. For subsequent experiments, the cells were seeded in 96-well plate, cover slip, and 60 mm Petri dish.

2.2 Preparation of liposomal celecoxib

Empty and celecoxib-loaded liposomes were prepared using modified thin film method as stated by Bangham et al. (Sadzuka et al. 2005). Briefly, phospholipid (DSPC) and celecoxib were dissolved together in methanol with the lipid to drug ratio of 4:1 *w/w* in a round-bottom flask. The solvent was then evaporated in a Bu̇chii rotoevaporator to form a thin film along the wall of the flask. It was attached to high vacuum for 2 h to remove any traces of the solvent. To the dry film, HEPES buffered saline (10 mM HEPES and 150 mM NaCl) was added and agitated above the gel transition temperature of DSPC. The liposomal suspension was then freeze-thawed for five times by alternately freezing in liquid nitrogen and then subsequently bringing above its gel transition temperature. The formed multilamellar vesicles were then sonicated using ultra sonic probe (Cole Parmer CP-18) for 20 min to obtain an optically clear solution. The resultant unilamellar vesicles were then centrifuged for 15 min at 4°C and 10,000 rpm to remove phospholipid residue and titanium impurity. The visibly clear supernatant was withdrawn and stored at 4°C. The liposomal solution was ultracentrifuged (Sorvall Ultra Pro 80) at 120,000×*g* force at 4°C for 2 h to remove any unencapsulated celecoxib. Supernatant was discarded, and pellet was resuspended in HEPES buffered saline (pH 7.0) to a final phospholipid concentration of 2 mg/ml. All experiments were performed with freshly prepared liposomes.

2.3 Analysis of liposomes using AFM and TEM

Vesicle formation and morphology of liposomes were analyzed using atomic force (AFM, Veeco CPII, USA) and high-resolution transmission electron (HRTEM, JEOL JEM) microscopies. The liposome samples were diluted (tenfold with 10 mM HEPES buffer saline), added to a freshly cleaved mica sheet and allowed to remain in contact for 5 min. From the mica sheet, excess sample was removed, dried, and analyzed using tapping mode AFM (Li et al. 2008; Nakano et al. 2008). The tapping mode settings were as follows—0.5 Hz scan rate, resolution of 256×256 data points per scan, AV-shaped silicon nitride cantilever (MMP-11123, Veeco Instruments Inc., USA) having spring constant 40 N/m, length 115–135 μm, and radii of curvature <10 nm.

For transmission electron microscopy (TEM) analysis, the diluted liposomes were applied to carbon-coated copper grids and negatively stained with 1% ammonium molybdate solution (pH 7.0). The excess of liposomes were

removed from the grid and dried for further analysis. Three grids were prepared for each sample.

2.4 Particle size and zeta potential measurement

The mean particle size, polydispersity index, and zeta potential of empty and celecoxib-loaded liposomes were measured by DLS (dynamic light scatter, Nano-ZS, Malvern Instrument, UK). HEPES buffered saline diluted liposome samples were backscattered by a helium-neon laser (633 nm) at an angle of 173° and temperature of 25°C (Zhang et al. 2008; Turanek et al. 2009; Yang et al. 2009). Mean surface charge was calculated from samples taken in triplicate and analyzed based on Gaussian size distribution.

2.5 Entrapment efficiency

A known volume of liposomal celecoxib was diluted into suitable concentration with methanol. It was then bath-sonicated to disrupt the liposomes and release the encapsulated celecoxib. The amount of encapsulated celecoxib in liposomes was quantitatively determined using reverse phase HPLC (Shimadzhu LC-10AD pump liquid chromatograph, Diamonsil® C-18 column, 250 mm×4.6 mm, 5 μm) using methanol/water (75:25 *v/v*) as mobile phase (Saha et al. 2002). The analysis was performed at 20 μl injection, 1.25 ml min^{-1} of flow rate, and UV detector at 250 nm (Baboota et al. 2007). Calibration curve was constructed using celecoxib in the concentration range of 0–150 μM. Dilution factor was taken into consideration for calculating the entrapment efficiency of celecoxib in liposomes. The analysis was done in triplicate, and values were reported as mean±SD. The percentage of celecoxib entrapped in liposomes was calculated as: Entrapment efficiency (%)=(Amount of encapsulated celecoxib/Total amount of celecoxib)×100.

2.6 Hemocompatibility study

Free celecoxib, empty, and celecoxib-loaded liposomes were diluted in 10 mM HEPES buffer saline to desired concentrations. Hemocompatibility of different samples were analyzed using a previous protocol with some modification (Katanasaka et al. 2008). In brief, blood was collected from 6-week-old BALB/c male mice and centrifuged (1,500×*g* for 5 min at 4°C using Ficoll density gradient solution) to obtain red blood cells (RBC). Collected RBC pellet was diluted with 20 mM HEPES buffered saline (pH 7.4) to give a 5% *v/v* solution. The RBC suspension was added to HEPES buffer saline, 1% Triton X-100, free celecoxib, and empty and celecoxib-loaded liposomes. All samples were incubated at 37°C for 30 and 60 min. After incubation, the samples were centrifuged at 12,000 rpm at 4°C, and supernatants were transferred to a 96-well plate. Hemolytic activity was determined by measuring the absorption at 570 nm (Bio-rad, microplate reader, model 550, Japan). Control samples of 0% lysis (in HEPES buffer) and 100% lysis (in 1% Triton X-100) were employed in the experiment (Guggi et al. 2004). The study was performed in triplicate. Hemolytic effect of each sample was expressed as percentage of cell lysis relative to the untreated control cells (% control) defined as: [(OD 570 nm sample)/(OD 570 nm control)]×100, where optical density was abbreviated to OD.

2.7 Cell proliferation assay

Cytotoxicity of free celecoxib, empty, and celecoxib-loaded liposomes on colon cancer cells HCT 15 was determined by cell proliferation assay as described previously (Yang et al. 2007). Briefly, HCT 15 cells in exponential growth phase were seeded onto 96-well plates at a density of 5×10^3 cells per well in 0.1 ml medium. Cells were allowed to adhere and grow for 24 h at 37°C in an incubator (Heraeus Hera Cell). Then, the medium was aspirated and replaced with 0.1 ml fresh medium containing various concentrations of free celecoxib, empty, and celecoxib-loaded liposomes. Control well was treated with equivalent volume of celecoxib-free media. After 72 h of incubation, the medium was removed, and cell viability was determined using a conventional MTT dye reduction assay. Then, 100 μl of 1 mg/ml MTT reagent was added to each well. After 4 h incubation, unreduced MTT solution was discarded. Then, 100 μl of dimethyl sulfoxide was added into each well to dissolve purple formazan crystals which was reduced from MTT by active mitochondria of viable cells. Plate was shaken for 20 min, and formazan dye was measured spectrophotometrically using a microplate reader. The experiment was performed in triplicate. The cytotoxicity of each treatment was expressed as percentage of cell viability relative to the untreated control cells (% control) defined as [(OD 550 nm treated cells)/(OD 550 nm control cells)]×100, where optical density is abbreviated to OD.

2.8 Morphological analysis

HCT 15 cells were grown at a density of 3×10^4 in Petri dishes and treated with absence (control) or presence of IC_{50} concentrations of free celecoxib, liposomal celecoxib, and empty liposomes (volume equivalent to liposomal celecoxib) for 48 h. After incubation, morphological changes were observed under phase contrast microscope (Leica, ×20; Caddeo et al. 2008).

Furthermore, morphological analysis of cancer cells using high-resolution scanning electron microscope (SEM) was performed to obtain a clear insight regarding

cell membrane extensions (filopodia and lamellipodia; Venkatesan et al. 2010). HCT 15 cells grown on a sterile cover slip were treated with free celecoxib (IC_{50}), liposomal celecoxib (IC_{50}), and empty liposomes (equivalent to volume liposomal celecoxib) for 48 h. Cells were washed thrice in 0.1 M cacodylate buffer (pH 7.4) and post-fixed using ice-cold 1% OsO_4 for 30 min. Cells were then dehydrated with grades (50%, 70%, 95%, and 100%) of ethanol. Next, the cover slips were placed in HMDS (1,1,1,3,3,3-hexamethyl disilazane) for 5 min to overcome drying effect. Samples were then air-dried at room temperature, mounted on a stub, and placed in vacuum chamber of SEM gold coating apparatus for gold coating (2.5 kV, 20–25 mA for 120 s). The morphogram of the HCT 15 cells was then observed using SEM (JEOL JSM-5800 Japan) at 20 kV acceleration voltage (Hodges 1970; Glaser et al. 1977).

2.9 Cell cycle analysis

HCT 15 cells at a density of 2×10^5 was cultured in 60 mm Petri dishes for 24 h and then treated with free celecoxib (IC_{50}), empty liposomes (equivalent to volume liposomal celecoxib), and celecoxib-loaded liposomes (IC_{50}) for 48 h. In this study, medium and empty liposome-treated cells were used as reference control and blank formulation, respectively. After incubation, HCT 15 cells were centrifuged at 1,200 rpm for 5 min at 4°C. The cell pellet was suspended in 5 ml of PBS and then centrifuged at 1,200 rpm for 10 min at 4°C. The supernatant was discarded, and the pellet was fixed with 2 ml of ice-cold ethanol solution (70% *v/v*) at 4°C overnight. Fixed cells were centrifuged at 1,200 rpm for 10 min at 4°C, and the pellet was incubated with PI mixture (10 mg/ml RNase, 20 μg/ml PI in cold PBS) for 30 min at 37°C. DNA content analysis was carried out on a FACS Calibur (BD Bioscience) flow cytometer (Celia et al. 2008). The data obtained were processed for cell cycle analysis with the Cell Quest Pro software package.

2.10 Nuclear analysis

Apoptosis of HCT 15 cells treated with free celecoxib, empty, and celecoxib-loaded liposomes was analyzed by epi-fluorescence microscopy. HCT 15 cells were seeded in six-well plates containing a cover slip with 2×10^5 cells per well and cultured at 37°C for 24 h. Cells were then treated with free celecoxib (IC_{50}), celecoxib-loaded liposomes (IC_{50}), and empty liposomes (equivalent to volume liposomal celecoxib) and culture medium (control) for 48 h. Cells were then fixed (2% ice-cold paraformaldehyde in PBS for 20 min), permeabilized (0.1% Triton X-100), stained (0.2 μg/ml DAPI in PBS for 15 min), and washed twice with PBS. Cover slips were mounted onto glass slides and examined using a fluorescence microscope (Leica DMR, ×20). Apoptotic cells were evaluated based on nuclear morphology, chromatin condensation, and fragmentation (Caddeo et al. 2008; Danhier et al. 2009).

2.11 Inhibition of DMBA-induced tumor in rat model

Female Wistar rats (6-week-old and 100 g of weight) were divided into five groups containing six rats each. Rats were maintained at 28±1°C, relative humidity at 60% (each 12 h of light and dark cycle). These rats were fed with standard food pellets (diet composition, broken wheat-moisture 9.0%, crude protein 11.5%, crude fat 1.9%, crude fiber 4.0%, Ash 0.2%, and nitrogen-free extract 73.4%) and tap water ad libitum. The experimental procedures were carried out with prior approval from animal ethical committee at the university.

2.11.1 Experimental design, tumor induction, and inhibition

Rat tumors were induced by DMBA injection (Huggins et al. 1961; Singh and Shukla 1998; Malejka-Giganti et al. 2000; Samy et al. 2006). DMBA (250 mg/kg) dissolved in 1 ml of vehicle (0.5 ml of sunflower oil plus 0.5 ml of PBS saline) was injected subcutaneously near either side of mammary glands. After 90 days of injection, tumor yield and size were stabilized.

Inhibition of DMBA-induced tumor by free celecoxib, empty, and celecoxib-loaded liposomes was determined. In this study, group (I) rats were fed with standard food pellet and tap water which served as a normal control. Rats with tumor (group II) were kept as cancer control. After 90 days of DMBA injection (after tumor formation), drug treatment was initiated. Furthermore, the tumor-bearing rat groups (II, III, IV, and V) were injected at tail vein with sterile PBS (cancer control), free celecoxib, empty, and celecoxib-loaded liposomes, respectively. Table 1 shows the dosage used in the experiment. All the groups were treated for three times in first 5 days and 1 day spaced between two injections. Rats were regularly examined for food and water consumption, apparent signs of toxicity and mortality for 30 days. At the end of the treatment period (after 120 days), total body weight of all rats was measured; they were starved overnight and sacrificed by cervical decapitation. The tumor was surgically dissected out and tumor volumes (Volume in cubic millimeter) of both the cancer and treatment groups were calculated with following formula: $V=(L\times W^2)/2$, where L (millimeters) is the longest diameter and W (millimeters) is perpendicular to L (Caddeo et al. 2008; Danhier et al. 2009).

2.12 Biochemical analysis of antioxidants

The following biochemical measurements were carried out in the rat liver and kidney tissues. The organs were

Table 1 Shows the experimental design, dosage, and treatment

Groups	Experimental design	Tumor induction (DMBA treatment 250 mg/ml/kg rat)	Tumor inhibition (treatment: three times in the first 5 days through tail vein injection, 1 day spaced between two administrations)
Group I	Normal control	–	–
Group II	Cancer control	Once/3 months	–
Group III	Cancer + celecoxib	Once/3 months	Celecoxib (100 μg/kg diluted in PBS)
Group IV	Cancer + empty liposome	Once/3 months	Empty liposome (equivalent volume of liposomal celecoxib) in PBS
Group V	Cancer + liposomal celecoxib	Once/3 months	Equivalent to celecoxib concentration 100 μg/kg in PBS

excised and removed from the experimental groups for the estimation of antioxidant enzymes. Tissues were washed thoroughly with ice-cold normal phosphate buffer saline, pH 7.2 (PBS, 0.9%) and cut into small pieces with a heavy-duty blade. Tissues were homogenized by a glass homogenizer tube in cold PBS, and centrifuged at 20,000 rpm for 10 min, and the supernatant was diluted with PBS up to a final protein concentration. Effects of liposomal celecoxib on activities of SOD generation and LPx were estimated in the liver and kidney tissues of treated and control rats.

2.12.1 SOD radical scavenging activity

SOD activity was assessed by the Nitroblue tetrazolium reduction method (Samy et al. 2006). Approximately, a known protein concentration of tissue supernatant was added to a reaction mixture containing 0.1 mM EDTA (200 μl), 0.12 mM riboflavin (50 μl), and 0.6 M phosphate buffer (pH 7.8) in a final volume of 3 ml. The optical density was measured at 560 nm.

2.12.2 Inhibition of LPx formation

Induction by Fe^{3+}/ascorbate system: the reaction mixture containing rat liver and kidney homogenate (0.1 ml, 50% *w/v*) in Tris–HCl (30 mM), ferrous ammonium sulfate (0.16 mM), ascorbic acid (0.06 mM), and the reaction mixture was incubated for 1 h at 37°C, and the resulting thiobarbituric reacting substances were measured (Samy et al. 2006). Briefly, a 0.4 ml aliquot of the reaction mixture was treated with sodium dodecyl sulfate (0.2 ml, 8%), thiobarbituric acid (1.5 ml, 0.8%), and acetic acid (1.5 ml, pH 3.5), made up to a total volume of 4 ml by adding distilled water, and then kept in a water bath at 95°C for 1 h. After cooling, 1 ml of distilled water and 5 ml of *n*-butanol/pyridine (15:1 *v/v*) were added. The organic layer was separated after shaking and centrifugation. LPx activity was measured in terms of thiobarbituric acid formation and the color intensity measured spectrophotometrically at 530 nm.

2.13 Statistical analysis

All the statistical analysis was performed by Graphpad Prism 5 software. Data were presented using mean±SD. The statistical significance was determined by using one-way analysis of variance (ANOVA). ***$P<0.001$ and **$P<0.05$ were considered significant.

3 Results and discussion

3.1 Analysis using AFM and TEM

The prepared liposomes appeared semi-transparent and visible sky-blue opalescent dispersion. Previous studies have reported that nature of phospholipid composition in liposomal carrier have influence on its stability, entrapment efficiency, and blood circulation time (Nakano et al. 2008). Furthermore, rigidity of liposome particles was attributed to phase transition temperature (55°C) of DSPC (Egawa and Furusawa 1999; Nakano et al. 2008). Our AFM images of both empty and celecoxib-loaded liposomes indicate spherical-shaped homogeneous particles (Fig. 1b–e).

In addition, TEM analysis is a semi-quantitative technique, which provides enough information on morphology of liposomes (Zhang et al. 2008). Under TEM analysis, surface morphology is very distinct with well-formed liposomes (Fig. 1f, g). The inner areas of both the liposomes appeared gloomy which might be attributed to dense packing of the lipid bilayer vesicles. The results displayed discrete, homogeneous, round particles with size of 125 and 170 nm for empty and celecoxib-loaded liposomes, respectively.

3.2 Particle size and zeta potential measurement

The DLS analysis showed mean particle size of 103.5 and 169 nm for empty and celecoxib-loaded liposomes, respectively. The results indicate formation of large unilamellar liposome formulation prepared by modified thin film method. Polydispersity index describes relative error

between curve fit and experimental values, which suggests homogeneity of colloidal suspension. Polydispersity index greater than 0.7 indicates that sample has a very broad size distribution (Caddeo et al. 2008). In our study, polydispersity index of empty and celecoxib-loaded liposomes was determined as 0.604 and 0.409, respectively, which indicate formation of homogeneous liposomes.

The zeta potential is a good index of degree of repulsive interactions between colloidal particles. It depends on particle composition, especially on the lipid concentration and incorporated drug (Katanasaka et al. 2008; Jung et al. 2009). Surface charge (zeta potential) measurement of empty and celecoxib-loaded liposomes have shown 0.11 and −8.22 mV, respectively. Since the phospholipid is almost neutral in charge, negative surface charge of celecoxib-loaded liposomes indicates likely association of celecoxib in liposomes. Furthermore, high negative charge of the liposomal celecoxib leads to high repulsive force between particles which might prevent aggregation liposome particles.

3.3 Entrapment efficiency of liposomes

The amount of celecoxib encapsulated in liposomes was determined by HPLC analysis. The study result shows 46% of entrapment efficiency, which indicates good incorporation potential of the prepared liposomes.

3.4 Hemocompatibility study

Intravenous administration of a drug is limited by properties like solubility, hemolysis, and toxicity. Liposomal formulations of hydrophobic drugs have been reported to overcome the solubility problem and hemolytic activity of free drugs (Guggi et al. 2004; Katanasaka et al. 2008). Hemolytic assay was performed to examine interaction between the anionic liposomal celecoxib and anionic red blood cell membrane (Katanasaka et al. 2008). The membrane-damaging property of liposomes was determined by measuring released hemoglobin.

To resolve whether liposomalization of celecoxib prevent hemolysis, the hemolytic assay was performed. Free celecoxib suspended in HEPES buffer saline induced significant hemolysis which might be attributed to SO_2NH_2 group present in celecoxib (Guggi et al. 2004). The interaction between the RBC and free celecoxib might induce membrane twist, cell rupture, and release of hemoglobin. However, empty and celecoxib-loaded liposomes exhibited significantly low hemolytic activities (Fig. 2a) that can be ascribed to rigidity of liposomes and electrostatic repulsion with anionic RBC (Nakano et al. 2008; Jung et al. 2009). Rigid molecules (e.g., DSPC) are less prone to attach to RBC membrane than flexible molecules, which would explain low hemolytic activities of both empty and celecoxib-loaded liposomes.

3.5 Cell proliferation assay

Compared with the free paclitaxel, liposomal formulation of paclitaxel has demonstrated enhanced solubility and cytotoxicity against variety of cancer cell lines (Yang et al. 2007). In this study, cytotoxicity of liposomal celecoxib and free celecoxib was investigated on HCT 15 cells using widely established metallothionein (MTT) assay. Both free

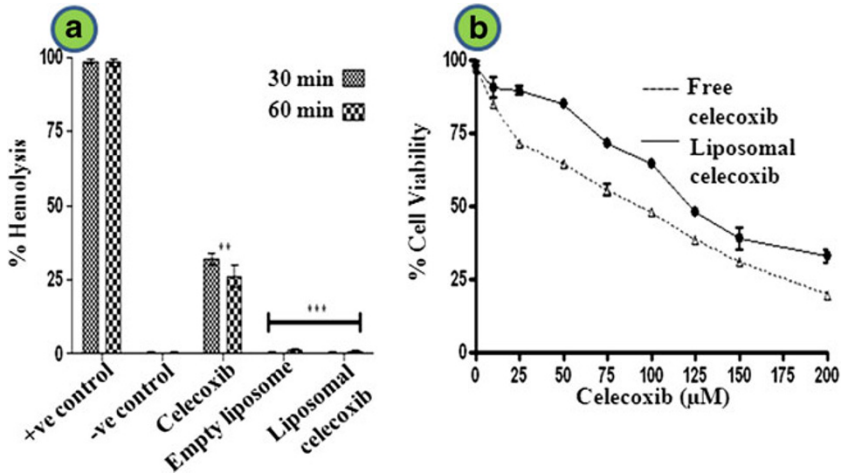

Fig. 2 **a** Hemolytic assay. In brief, red blood cells were collected by centrifugation of mice blood and resuspended in HEPES buffer saline (5% *v/v*). The cell suspension was added to HEPES buffer saline, 1% Triton X-100, free celecoxib, and empty and celecoxib-loaded liposomes, and incubated for 30 and 60 min at 37°C. After centrifugation, hemolytic activity was determined by measuring the absorbance of the supernatants at 570 nm. Control samples of 0% lysis (in HEPES buffer) and 100% lysis (in 1% Triton X-100) were used in the experiment. The *bars* indicate the mean±SD (n=3). Significant difference is shown as $^{**}p<0.05$; $^{***}p<0.001$ versus + control. **b** Antiproliferative activity of free celecoxib and liposomal celecoxib on HCT 15 cells. Each point in the graph indicates the mean±SD (n=3)

celecoxib and liposomal celecoxib have significantly inhibited HCT 15 cells proliferation in a dose-dependent manner. The IC_{50} value of the free celecoxib on HCT 15 cell was a little lower (102.71 μM) than liposomal celecoxib (IC_{50} 127.67 μM; Venkatesan et al. 2010). Furthermore, free celecoxib displayed low cell viability compared with liposomal celecoxib which might be due to higher intracellular uptake of free celecoxib by HCT 15 cells (Fig. 2b; Caddeo et al. 2008; Celia et al. 2008; Abu Lila et al. 2009). In contrast, low cytotoxicity mediated by liposomal celecoxib might be ascribed to low intracellular uptake resulting from electrostatic repulsion between cells (anionic) and liposomes (anionic), and slow release of celecoxib. This results in reduced intracellular concentration of celecoxib in the cells. As expected, the empty liposomes did not show growth inhibitory activity on HCT 15 cells at volume equivalent to the celecoxib-loaded liposomes (data not shown). This observation substantiates that the cytotoxicity of liposomal celecoxib on HCT 15 cells is due to the celecoxib released from liposomes than the carrier itself (phospholipid).

3.6 Morphological analysis

Morphological analysis of HCT 15 cells treated with free celecoxib, empty, and celecoxib-loaded liposomes was performed using phase contrast microscope (Leica, ×20). The control HCT 15 cells displayed confluent monolayer, and elongated and flattened cell morphology (Fig. 3a). Furthermore, empty liposome-treated HCT 15 cells exhibited proliferated cell with no significant morphological changes. In contrast, free celecoxib- and liposomal celecoxib-treated HCT 15 cells have shown significant morphological changes which include small group of shrunken and retracted cells from substratum.

SEM is a vital tool to analyze surface and morphological features of cancer cells. Many researchers have used SEM for morphological analysis of normal and cancer cells (Jacobs et al. 1976). SEM analysis of osteosarcoma has revealed a close relationship between cell morphology and its function (Docheva et al. 2008). Previous study of AEE788- and/or celecoxib-mediated morphological changes used SEM to evaluate the anticancer activity. Anticancer agent-mediated morphological changes in cancer cell may potentially be valuable for cancer chemotherapy (Venkatesan et al. 2010). The study was aimed to analyze morphology of celecoxib, empty, and celecoxib-loaded liposome-treated HCT 15 cells. From the obtained SEM image (Fig. 3b), the control HCT 15 cells have shown highly dynamic, flat cell with filamentous lateral cell membrane extensions (filopodia and lamellipodia). In contrast, free celecoxib- and liposomal celecoxib-treated HCT 15 cells have demonstrated shrunken morphology, small ruffles, irregular cytoplasm

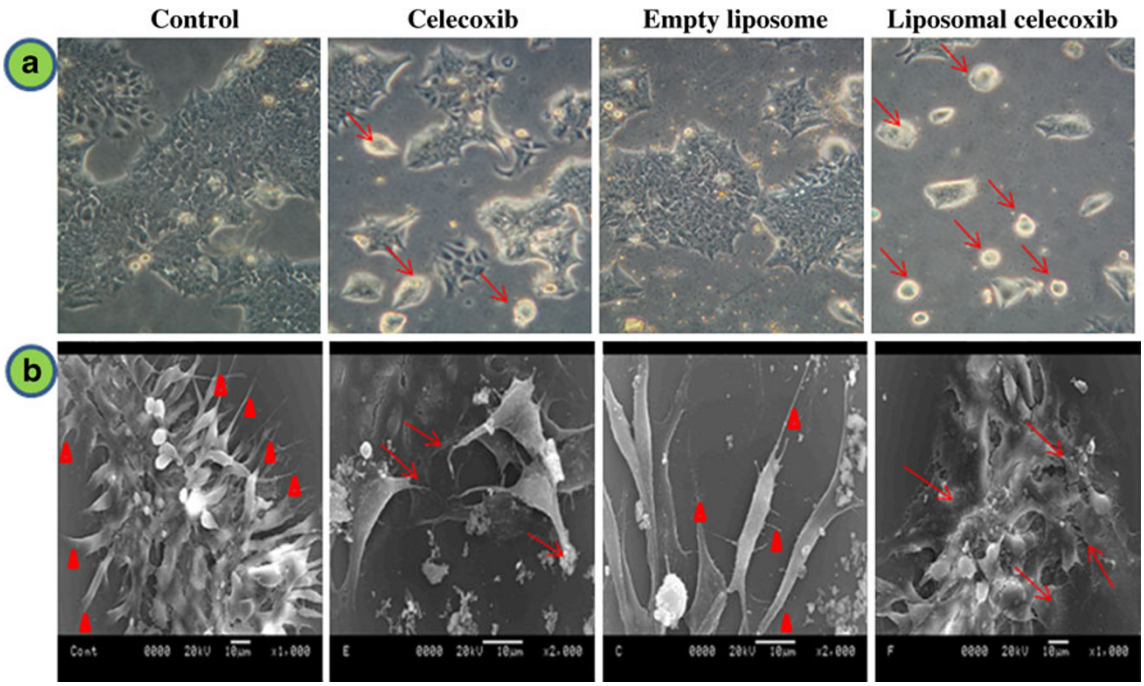

Fig. 3 **a** Phase contrast microscopic and **b** scanning electron microscopic images of HCT 15 cells treated with control, free celecoxib (IC_{50}), liposomal celecoxib (IC_{50}), and empty liposomes (equivalent to volume of liposomal celecoxib) for 48 h. **a** In phase contrast microscopic images, the apoptotic cells are marked with *arrows*. All images were taken under the identical instrumental conditions and presented at the same intensity scale. **b** In SEM images, healthy filopodia and lamellipodia are marked with *arrowheads* and truncated lamellipodia and filopodia are marked with *arrows*

detached from substratum, and loss of cell membrane extensions. However, empty liposome-treated HCT 15 cells showed insignificant changes in cell morphology. It was observed that the cytotoxicity of liposomal celecoxib on HCT 15 cells was equivalent to free celecoxib. All the above results suggest the liposomes nanocarriers could be a promising choice for celecoxib delivery without loss of its therapeutic efficacy.

3.7 Cell cycle analysis

Apoptosis fraction was considered as DNA loss resulting in sub-G1 peak which can be analyzed by flow cytometry. The amount of PI intercalating to DNA was used as parameter to determine the cell cycle distribution phases. To find mechanism of apoptosis mediated by free celecoxib and liposomal celecoxib, cell cycle analysis was performed to check the changes in sub-G1 peak. HCT 15 cells were treated with free celecoxib, empty, and celecoxib-loaded liposomes for 48 h and subjected to flow cytometric analysis. The empty liposome-treated HCT 15 cells did not show significant apoptosis (1.53± 0.47%) which is insignificant compared with control treatment (0.92±0.34%; Fig. 4a). In case of free celecoxib and liposomal celecoxib, treatment resulted in 34.14±0.47% and 24.21±0.75% of apoptosis, respectively (Fig. 4a). Results indicate that the apoptosis induced by liposomal celecoxib was slightly lower than free celecoxib treatment. This might be due to lower intracellular level of liposomal celecoxib and slow release of celecoxib from liposomes. Increased apoptosis of free celecoxib treatment results from increased availability or intracellular concentrations of celecoxib in HCT 15 cells (Celia et al. 2008).

3.8 Epi-fluorescence microscopic analysis

The majority of anticancer agents including celecoxib interact with nuclear DNA to cause DNA damage thus preventing cell proliferation and inducing apoptosis (Wei et al. 2008; Danhier et al. 2009; Jung et al. 2009; Munoz-Bonilla et al. 2009; Yuan et al. 2010). The control and treated HCT 15 cells were stained with DAPI. The control HCT 15 cells displayed normal, round nuclear morphology, and homogenous fluorescence without any DNA fragmentation. In a similar way, the empty liposome-treated HCT 15 cells have also displayed no sign of DNA damage (Fig. 4b). This further substantiates biocompatibility of the liposomal carrier. Conversely, free celecoxib- and liposomal celecoxib-treated HCT 15 cells have displayed typical morphological characteristics of apoptosis which include shrunken nuclear size, chromatin condensation, and much brighter nuclear fragmentation compared with control. The ability of liposomal celecoxib to induce apoptosis suggests that the liposomalization did not affect apoptosis induction by celecoxib.

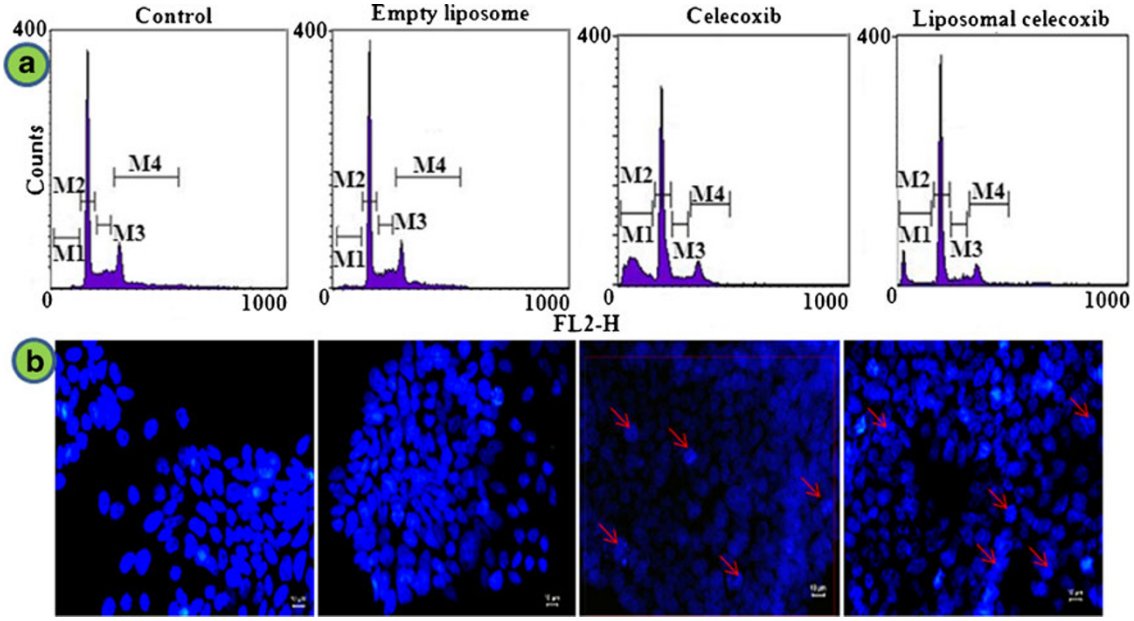

Fig. 4 **a** Cell cycle analysis of HCT 15 cells treated with control (PBS), celecoxib (IC_{50}), empty liposomes (equivalent to volume of liposomal celecoxib), and liposomal celecoxib (IC_{50}) for 48 h. M1-Sub-G1 Phase, M2-G0/G1 Phase, M3-S Phase, and M4-G2/M Phase. **b** DAPI nuclear staining of HCT 15 cells treated with control, free celecoxib (IC_{50}), empty liposomes (equivalent to volume of liposomal celecoxib), and liposomal celecoxib (IC_{50}) for 48 h (epi-fluorescence microscopic image at ×20 and scale bars, 10 μm). DNA fragmentation and apoptosis are marked with *arrows*

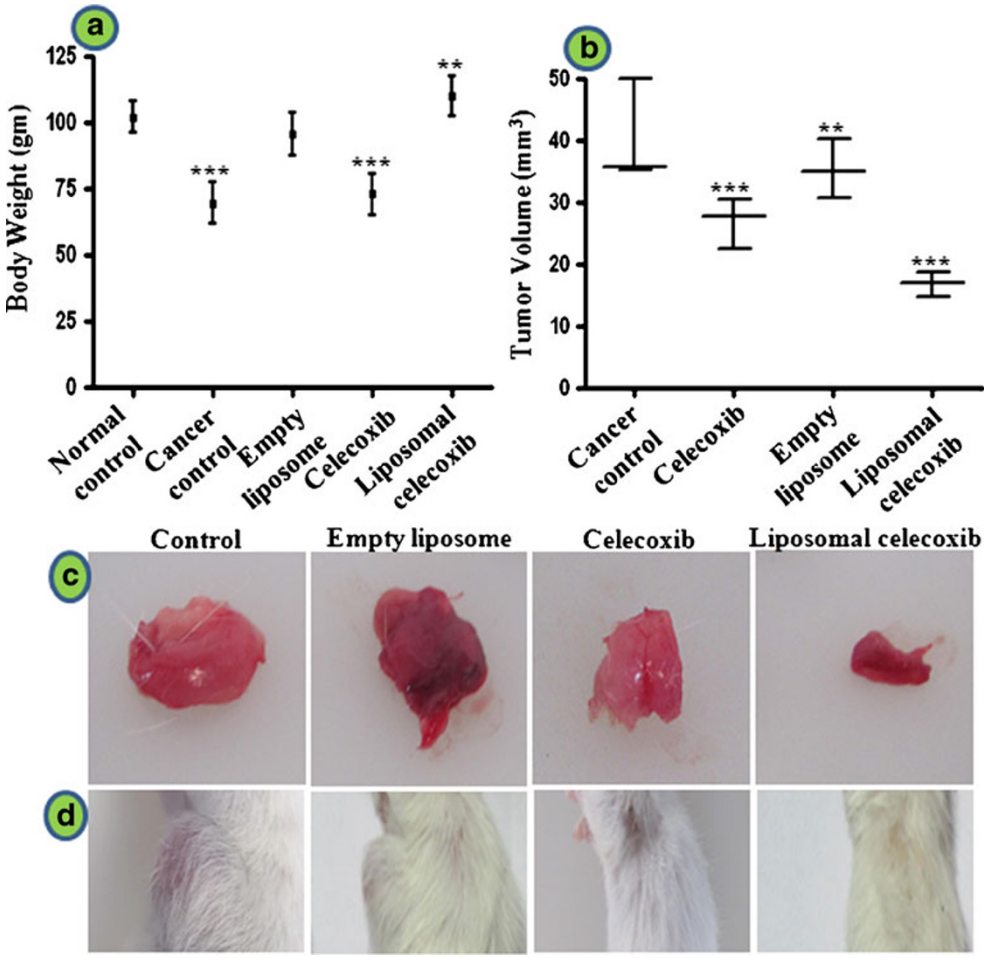

Fig. 5 Effect of PBS (*control*), free celecoxib, empty liposomes, and liposomal celecoxib on DMBA-induced rat tumor model. Body weight loss of treated groups compared with control (n=6) (**a**). Decrease in tumor volume (cubic millimeters) after 30 days of treatment (tumor induction 90 days+ treatment 30 days=120 days) (**b**). The images of dissected tumor before and after 30 days post-treatment (**c**). The images of the tumors in rat model were shown (**d**). The results were presented as mean±SD (n=3). ***P<0.001; **P<0.05, when compared with control group. All images were taken under the identical instrumental conditions and presented at the same intensity scale

3.9 Inhibition of DMBA-induced tumor in rat model

In this study, tumors in reversible stage (90 days after injection of DMBA) were used (Samy et al. 2006). The maximum tolerated dose of celecoxib in rodents has been reported as 1 mg/kg of body weight (Paulson et al. 2000). Figure 5a–c shows changes in body weight, tumor volume, and dissected tumors before and after treatment, respectively. Compared with negative control (group I), the untreated tumor-bearing control (group II) displayed decrease in body weight. Group III treated with free celecoxib resulted in significant decrease in tumor volume compared with control cancer (group II; Fig. 5b). But the reduction was less than liposomal celecoxib treatment which can be attributed reduced availability of celecoxib at tumor site and less half life of celecoxib in blood. Decrease in body weight after celecoxib treatment might be due to toxicity associated with celecoxib and weakness

Table 2 The effect of liposomal celecoxib on antioxidant enzymes of liver in DMBA-induced cancer in rats

Groups	Treatment groups	Superoxide dismutase	Lipid peroxidation
Group I	Normal control	3.45±0.07*	0.79±0.06*
Group II	Cancer control	1.27±0.17	1.95±0.27
Group III	Cancer + celecoxib	2.31±0.29*	0.71±0.06*
Group IV	Cancer + empty liposome	1.39±0.37	1.77±0.47*
Group V	Cancer + liposomal celecoxib	3.35±0.21*	1.09±0.08*

Each value represents mean±SD of given number of animals (n=4); comparison groups I, III, IV, and V with group II

*P<0.01, significant values

Table 3 The effect of liposomal celecoxib on antioxidant enzymes of kidney in DMBA-induced cancer in rats

Groups	Treatment	Superoxide dismutase	Lipid peroxidation
Group I	Normal control	1.55±0.20*	1.70±0.33*
Group II	Cancer control	0.69±0.08	2.68±0.24
Group III	Cancer + celecoxib	1.36±0.12*	1.91±0.40*
Group IV	Cancer + empty liposome	1.09±0.20*	2.15±0.24*
Group V	Cancer + liposomal celecoxib	1.18±0.08*	1.69±0.18*

Each value represents mean±SD of given number of animals (n=4); comparison groups I, III, IV, and V with group II

*P<0.01, significant values

in rat after tumor progression. Treatment using empty liposomes (group IV) produced no significant change in tumor volume. In case of rats (group V) treated with liposomal celecoxib, there was significant decrease in tumor volume with minimal or no change in total body weight compared to control and other treated groups. It is suggested that higher concentration of celecoxib at the tumor site might be attained through EPR effect upon liposomal celecoxib treatment. This resulted in prominent reduction in tumor volume and toxicity (insignificant change in body weight). We have also observed that the tumors in control and empty liposome-treated groups became ulcerated at the end of 120 days, possibly due to aggressive growth (Fig. 5d). The liposomal celecoxib-treated rat (group V) displayed no ulceration and tumor-induced mortality when compared with the control (group II).

3.10 Antioxidant activity

Reactive oxygen species (ROS) are involved in a variety of important pathological conditions including tumerogenesis. Free radicals play vital role in tumor promotion by alteration of cellular metabolic processes and their scavengers (SOD and LPx). These scavengers inhibit tumorogenesis which involve in the biotransformation and detoxification of carcinogens at cytosol and mitochondria. Previous studies have shown that anticancer agents mediate apoptosis in colon cancer cell through suppression of ROS (Ling et al. 2003). Free radical scavengers SOD acts as a carcinogen inhibitor during initiation and promotion/transformation stages of carcinogenesis (Samy et al. 2006). The effect of liposomal celecoxib in activation of antioxidant enzymes was analyzed in liver and kidney tissues. In vitro analysis of influences of liposomal celecoxib on free radical scavenger enzymes were estimated in the liver supernatants (Table 2). Results showed significantly elevated levels of SOD in liposomal celecoxib-treated group compared with cancer control group. Decreased level of antioxidants in cancer-bearing animals indicates of oxidative stress, which may be the cause of lipid peroxidation-induced DNA damage. The LPx level of cancer control was increased from normal control. However, the potential reduction of LPx was observed in the liposomal celecoxib-treated groups which was comparable to normal control.

SOD and LPx were also recorded in kidney supernatants (Table 3). The activity of SOD has been increased in the kidneys of cancer-bearing rats treated with liposomal celecoxib compared with the untreated rat group. LPx level was very much influenced by the carcinogen (DMBA) in the cancer control group. However, the significant reduction of LPx was observed in the liposomal celecoxib-treated group, and it was comparable to the normal control group. The liposomal celecoxib treatment inhibits the tumor cell growth by antioxidant enzymes which directly resist the oxidant attack and may protect cells against lipid peroxidation and DNA damage.

4 Conclusions

This study presents the preparation of liposomal celecoxib formulation and its effect on colon cancer in vitro and DMBA-induced cancer in vivo models. The fundamental outcome of the study is the successful formation of liposomal celecoxib with appropriate size, high entrapment efficiency, and hemocompatibility. Liposomal celecoxib- and free celecoxib-mediated cytotoxicity and apoptosis on HCT 15 cells are comparable. In addition, in vivo study exhibited more potent tumor growth inhibition by liposomal celecoxib than free celecoxib in rat tumor model without producing mortality and side effects. These results suggest that the liposome carriers may serve as an effective and safe vehicle for celecoxib delivery in colon cancer chemotherapy. This preliminary approach of liposome-mediated targeted delivery might overcome side effects caused by celecoxib. In this regard, detailed preclinical studies are required before advancing into human application.

Acknowledgments This work was supported by funds from the School of Medical Science and Technology, Indian Institute of Technology, Kharagpur, India. We are grateful to Aarthi Drug Ltd., Mumbai, for generously providing celecoxib.

References

Abu Lila AS, Kizuki S, Doi Y, Suzuki T, Ishida T, Kiwada H (2009) Oxaliplatin encapsulated in PEG-coated cationic liposomes induces significant tumor growth suppression via a dual-targeting approach in a murine solid tumor model. J Control Release 137:8–14

Auman JT, Church R, Lee SY, Watson MA, Fleshman JW, McLeod HL (2008) Celecoxib pre-treatment in human colorectal adenocarcinoma patients is associated with gene expression alterations suggestive of diminished cellular proliferation. Eur J Cancer 44:1754–1760

Baboota S, Al-Azaki A, Kohli K, Ali J, Dixit N, Shakeel F (2007) Development and evaluation of a microemulsion formulation for transdermal delivery of terbinafine. PDA J Pharm Sci Technol 61:276–285

Bijman MN, Hermelink CA, van Berkel MP, Laan AC, Janmaat ML, Peters GJ, Boven E (2008) Interaction between celecoxib and docetaxel or cisplatin in human cell lines of ovarian cancer and colon cancer is independent of COX-2 expression levels. Biochem Pharmacol 75:427–437

Caddeo C, Teskac K, Sinico C, Kristl J (2008) Effect of resveratrol incorporated in liposomes on proliferation and UV-B protection of cells. Int J Pharm 363:183–191

Celia C, Malara N, Terracciano R, Cosco D, Paolino D, Fresta M, Savino R (2008) Liposomal delivery improves the growth-

inhibitory and apoptotic activity of low doses of gemcitabine in multiple myeloma cancer cells. Nanomedicine 4:155–166
Danhier F, Lecouturier N, Vroman B, Jerome C, Marchand-Brynaert J, Feron O, Preat V (2009) Paclitaxel-loaded PEGylated PLGA-based nanoparticles: in vitro and in vivo evaluation. J Control Release 133:11–17
Dhawan D, Jeffreys AB, Zheng R, Stewart JC, Knapp DW (2008) Cyclooxygenase-2 dependent and independent antitumor effects induced by celecoxib in urinary bladder cancer cells. Mol Cancer Ther 7:897–904
Docheva D, Padula D, Popov C, Mutschler W, Clausen-Schaumann H, Schieker M (2008) Researching into the cellular shape, volume and elasticity of mesenchymal stem cells, osteoblasts and osteosarcoma cells by atomic force microscopy. J Cell Mol Med 12:537–552
Drummond DC, Meyer O, Hong K, Kirpotin DB, Papahadjopoulos D (1999) Optimizing liposomes for delivery of chemotherapeutic agents to solid tumors. Pharmacol Rev 51:691–743
Egawa H, Furusawa K (1999) Liposome adhesion on mica surface studied by atomic force microscopy. Langmuir 15:1660–1666
Gaiser T, Becker MR, Habel A, Reuss DE, Ehemann V, Rami A, Siegelin MD (2008) TRAIL-mediated apoptosis in malignant glioma cells is augmented by celecoxib through proteasomal degradation of survivin. Neurosci Lett 442:109–113
Glaser R, Mumaw V, Farrugia R, Munger B (1977) Scanning electron microscopy of the surfaces of hamster embryo cells transformed by herpes simplex virus. Cancer Res 37:4420–4422
Guggi D, Langoth N, Hoffer MH, Wirth M, Bernkop-Schnurch A (2004) Comparative evaluation of cytotoxicity of a glucosamine-TBA conjugate and a chitosan-TBA conjugate. Int J Pharm 278:353–360
Hiremath PS, Soppimath KS, Betageri GV (2009) Proliposomes of exemestane for improved oral delivery: formulation and in vitro evaluation using PAMPA, Caco-2 and rat intestine. Int J Pharm 380:96–104
Hodges GM (1970) A scanning electron microscope study of cell surface and cell contacts of "spontaneously" transformed cells in vitro. Eur J Cancer 6:235–239
Hsiao PW, Chang CC, Liu HF, Tsai CM, Chiu TH, Chao JI (2007) Activation of p38 mitogen-activated protein kinase by celecoxib oppositely regulates survivin and gamma-H2AX in human colorectal cancer cells. Toxicol Appl Pharmacol 222:97–104
Huggins C, Grand LC, Brillantes FP (1961) Mammary cancer induced by a single feeding of polymucular hydrocarbons, and its suppression. Nature 189:204–207
Jacobs JB, Arai M, Cohen SM, Friedell GH (1976) Early lesions in experimental bladder cancer: scanning electron microscopy of cell surface markers. Cancer Res 36:2512–2517
Jung SH, Seong H, Cho SH, Jeong KS, Shin BC (2009) Polyethylene glycol-complexed cationic liposome for enhanced cellular uptake and anticancer activity. Int J Pharm 382:254–261
Katanasaka Y, Ida T, Asai T, Shimizu K, Koizumi F, Maeda N, Baba K, Oku N (2008) Antiangiogenic cancer therapy using tumor vasculature-targeted liposomes encapsulating 3-(3,5-dimethyl-1H-pyrrol-2-ylmethylene)-1,3-dihydro-indol-2-one, SU5416. Cancer Lett 270:260–268
Li Q, Peng J, Zhang GY (2008) Effect of a selective COX-2 inhibitor on cell proliferation and apoptosis in human gastric cancer cell line BGC-823. Zhong Nan Da Xue Xue Bao Yi Xue Ban 33:1123–1128
Ling YH, Liebes L, Zou Y, Perez-Soler R (2003) Reactive oxygen species generation and mitochondrial dysfunction in the apoptotic response to Bortezomib, a novel proteasome inhibitor, in human H460 non-small cell lung cancer cells. J Biol Chem 278:33714–33723
Lu Y, Li J, Wang G (2008) In vitro and in vivo evaluation of mPEG-PLA modified liposomes loaded glycyrrhetinic acid. Int J Pharm 356:274–281
Maier TJ, Schilling K, Schmidt R, Geisslinger G, Grosch S (2004) Cyclooxygenase-2 (COX-2)-dependent and -independent anti-carcinogenic effects of celecoxib in human colon carcinoma cells. Biochem Pharmacol 67:1469–1478
Malejka-Giganti D, Niehans GA, Reichert MA, Bliss RL (2000) Post-initiation treatment of rats with indole-3-carbinol or beta-naphthoflavone does not suppress 7, 12-dimethylbenz[a]anthracene-induced mammary gland carcinogenesis. Cancer Lett 160:209–218
Mazhar D, Ang R, Waxman J (2006) COX inhibitors and breast cancer. Br J Cancer 94:346–350
Mohammed SI, Dhawan D, Abraham S, Snyder PW, Waters DJ, Craig BA, Lu M, Wu L, Zheng R, Stewart J, Knapp DW (2006) Cyclooxygenase inhibitors in urinary bladder cancer: in vitro and in vivo effects. Mol Cancer Ther 5:329–336
Munoz-Bonilla A, Ibarboure E, Papon E, Rodriguez-Hernandez J (2009) Self-organized hierarchical structures in polymer surfaces: self-assembled nanostructures within breath figures. Langmuir 25:6493–6499
Nakano K, Tozuka Y, Yamamoto H, Kawashima Y, Takeuchi H (2008) A novel method for measuring rigidity of submicron-size liposomes with atomic force microscopy. Int J Pharm 355:203–209
Paulson SK, Zhang JY, Breau AP, Hribar JD, Liu NW, Jessen SM, Lawal YM, Cogburn JN, Gresk CJ, Markos CS, Maziasz TJ, Schoenhard GL, Burton EG (2000) Pharmacokinetics, tissue distribution, metabolism, and excretion of celecoxib in rats. Drug Metab Dispos 28:514–521
Paulson SK, Vaughn MB, Jessen SM, Lawal Y, Gresk CJ, Yan B, Maziasz TJ, Cook CS, Karim A (2001) Pharmacokinetics of celecoxib after oral administration in dogs and humans: effect of food and site of absorption. J Pharmacol Exp Ther 297:638–645
Sadzuka Y, Takabe H, Sonobe T (2005) Liposomalization of SN-38 as active metabolite of CPT-11. J Control Release 108:453–459
Saha RN, Sajeev C, Jadhav PR, Patil SP, Srinivasan N (2002) Determination of celecoxib in pharmaceutical formulations using UV spectrophotometry and liquid chromatography. J Pharm Biomed Anal 28:741–751
Sakoguchi-Okada N, Takahashi-Yanaga F, Fukada K, Shiraishi F, Taba Y, Miwa Y, Morimoto S, Iida M, Sasaguri T (2007) Celecoxib inhibits the expression of survivin via the suppression of promoter activity in human colon cancer cells. Biochem Pharmacol 73:1318–1329
Samy RP, Gopalakrishnakone P, Ignacimuthu S (2006) Anti-tumor promoting potential of luteolin against 7,12-dimethylbenz(a) anthracene-induced mammary tumors in rats. Chem Biol Interact 164:1–14
Singh A, Shukla Y (1998) Antitumour activity of diallyl sulfide on polycyclic aromatic hydrocarbon-induced mouse skin carcinogenesis. Cancer Lett 131:209–214
Storm G, Roerdink FH, Steerenberg PA, de Jong WH, Crommelin DJ (1987) Influence of lipid composition on the antitumor activity exerted by doxorubicin-containing liposomes in a rat solid tumor model. Cancer Res 47:3366–3372
Tan ML, Friedhuber AM, Dunstan DE, Choong PF, Dass CR (2010) The performance of doxorubicin encapsulated in chitosan-dextran sulphate microparticles in an osteosarcoma model. Biomaterials 31:541–551
Turanek J, Wang XF, Knotigova P, Koudelka S, Dong LF, Vrublova E, Mahdavian E, Prochazka L, Sangsura S, Vacek A, Salvatore BA, Neuzil J (2009) Liposomal formulation of alpha-tocopheryl maleamide: in vitro and in vivo toxicological profile and anticancer effect against spontaneous breast carcinomas in mice. Toxicol Appl Pharmacol 237:249–257

Venkatesan P, Das S, Krishnan MM, Chakraborty C, Chaudhury K, Mandal M (2010) Effect of AEE788 and/or Celecoxib on colon cancer cell morphology using advanced microscopic techniques. Micron 41:247–256

Wei W, Ma GH, Hu G, Yu D, McLeish T, Su ZG, Shen ZY (2008) Preparation of hierarchical hollow CaCO3 particles and the application as anticancer drug carrier. J Am Chem Soc 130:15808–15810

Yang T, Cui FD, Choi MK, Cho JW, Chung SJ, Shim CK, Kim DD (2007) Enhanced solubility and stability of PEGylated liposomal paclitaxel: in vitro and in vivo evaluation. Int J Pharm 338:317–326

Yang X, Zhao X, Phelps MA, Piao L, Rozewski DM, Liu Q, Lee LJ, Marcucci G, Grever MR, Byrd JC, Dalton JT, Lee RJ (2009) A novel liposomal formulation of flavopiridol. Int J Pharm 365:170–174

Yuan Y, Liu C, Qian J, Wang J, Zhang Y (2010) Size-mediated cytotoxicity and apoptosis of hydroxyapatite nanoparticles in human hepatoma HepG2 cells. Biomaterials 31:730–740

Zhang L, Gao H, Chen L, Wu B, Zheng Y, Liao R, Jiang Y, He F (2008) Tumor targeting of vincristine by mBAFF-modified PEG liposomes in B lymphoma cells. Cancer Lett 269:26–36